

Major deep levels with the same microstructures observed in n-type 4H-SiC and 6H-SiC

S. Sasaki,^{a)} K. Kawahara, G. Feng, G. Alfieri, and T. Kimoto

Department of Electronic Science and Engineering, Kyoto University, Katsura, Nishikyo, Kyoto 615-8510, Japan

(Received 15 October 2010; accepted 16 November 2010; published online 5 January 2011)

Major deep levels observed in as-grown and irradiated n-type 4H-SiC and 6H-SiC epilayers have been investigated. After low-energy electron irradiation, by which only carbon atoms are displaced, five traps, EH1 ($E_C-0.36$ eV), Z_1/Z_2 ($E_C-0.65$ eV), EH3 ($E_C-0.79$ eV), EH5 ($E_C-1.0$ eV), and EH6/7 ($E_C-1.48$ eV), were detected in 4H-SiC and four traps, E_1/E_2 ($E_C-0.45$ eV), RD_5 ($E_C-0.57$ eV), ES ($E_C-0.80$ eV), and R ($E_C-1.25$ eV), were detected in 6H-SiC. The Z_1/Z_2 , EH6/7 centers in 4H-SiC and the E_1/E_2 , R centers in 6H-SiC exhibit common features as follows: their generation rates by the e^- -irradiation were almost the same each other, their concentrations were not changed by heat treatments up to 1500 °C, and they showed very similar annealing behaviors at elevated temperatures. Furthermore, these defect centers were almost eliminated by thermal oxidation. Taking account of the observed results and the energy positions, the authors suggest that the Z_1/Z_2 center in 4H-SiC corresponds to the E_1/E_2 center in 6H-SiC, and the EH6/7 center in 4H-SiC to the R center in 6H-SiC, respectively. Since the concentrations of these four centers are almost the same for as-grown, electron-irradiated, annealed, and oxidized samples, these centers will contain a common intrinsic defect, most likely carbon vacancy. The authors also observed similar correspondence for other thermally unstable traps in 4H-SiC and 6H-SiC. © 2011 American Institute of Physics. [doi:10.1063/1.3528124]

I. INTRODUCTION

SiC is an attractive material for high-power, high-temperature, and high-frequency operating devices.^{1,2} Among many SiC polytypes, 4H-SiC is regarded as the most suitable polytype for such device applications owing to its large band gap, high electron mobility, and small anisotropy. However, the presence of various defects has so far hindered SiC-based device commercialization in a large scale. Deep levels in semiconductors have several harmful effects such as carrier trapping, increase in leakage current, and reduction in minority carrier lifetimes. In as-grown n-type 4H-SiC, the Z_1/Z_2 center³ and the EH6/7 center⁴ are dominant traps. The Z_1/Z_2 center has been identified as a dominant lifetime-killing defect in n-type 4H-SiC.⁵⁻⁸ The Z_1/Z_2 and EH6/7 centers are frequently generated during device processes such as ion implantation or high-temperature annealing. From previous deep level transient spectroscopy (DLTS) studies, it was suggested that the Z_1/Z_2 and EH6/7 centers may originate from a similar microstructure⁹ and may be related to a carbon vacancy.^{9,10}

Each point defect must have different activation energies in different SiC polytypes. Only a few reports can be found on the comparative study of deep levels in different SiC polytypes. Pensl and co-workers suggested that the Z_1/Z_2 center in 4H-SiC and the E_1/E_2 center in 6H-SiC may originate from the same point defect.^{11,12} They observed identical temperature dependence of these trap concentrations. Hemmingsson *et al.* demonstrated that both traps have negative-U properties.^{13,14} For these traps, the thermal barrier for elec-

tron capturing is close to zero or very small.^{4,15} In this study, the major deep levels observed in as-grown and irradiated n-type 4H-SiC and 6H-SiC epilayers have been systematically investigated using DLTS. The samples were irradiated with electrons at an energy of 150 keV with various fluences. By such low-energy e^- -irradiation, only carbon atom displacement can take place in SiC crystals.¹⁰ Although several groups studied radiation-induced defects in 6H-SiC,^{3,11,12,15-21} there are no reports on deep levels in 6H-SiC irradiated with such low-energy electrons. In this study, the authors detected several traps in both 4H-SiC and 6H-SiC after the e^- -irradiation. Their generation rates by the e^- -irradiation and their annealing behaviors are compared. In addition, the authors investigate effects of thermal oxidation on deep levels. So far, impacts of thermal oxidation on the deep levels in 6H-SiC have not been investigated. Based on these results, the microscopic nature as well as the energy levels of deep levels in different SiC polytypes are discussed.

II. EXPERIMENTS

The starting materials were N-doped n-type 4H-SiC epilayers grown on 8° off-axis 4H-SiC (0001) and N-doped n-type 6H-SiC epilayers grown on 3.3° off-axis 6H-SiC (0001).²² The thickness and doping concentration of the epilayers were 10–15 μm and 5×10^{15} – 1×10^{16} cm^{-3} , respectively. Electron irradiation was performed at an energy of 150 keV without intentional heating. The electron fluence was varied from 1×10^{16} to 4×10^{17} cm^{-2} . DLTS spectra were obtained in the temperature range of 150–700 K before and after the e^- -irradiation. For the DLTS measurements, nickel was evaporated onto the sample surface as Schottky

^{a)}Electronic mail: sasaki@semicon.kuee.kyoto-u.ac.jp.

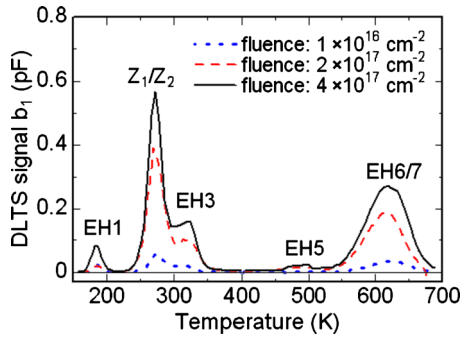


FIG. 1. (Color online) DLTS spectra of as-irradiated n-type 4H-SiC. Electron irradiation was performed at an energy of 150 keV with fluences of 1×10^{16} , 2×10^{17} , and $4 \times 10^{17} \text{ cm}^{-2}$.

contacts with a thickness of approximately 80 nm. The typical reverse bias and pulse voltages were -5 V and 0 V , respectively. In this study, a Fourier transform analysis of the measured transients was employed,²³ and temperature-independent capture cross section was assumed when analyzing the DLTS data. After the DLTS measurements on as-irradiated samples, Ni Schottky contacts were removed for the annealing experiment. The samples were annealed in Ar ambient for 30 min at temperature from 950 to 1750 °C. A rapid thermal annealing furnace was used for 950 °C annealing. For annealing above 950 °C, carbon cap was employed to suppress the surface roughening,²⁴ and a hot-wall chemical vapor deposition chamber was used. After the DLTS measurements on the annealed samples, Ni Schottky contacts were removed again, and then thermal oxidation was carried out in dry O_2 ambient at 1150 °C for 6 h. The oxides were removed by hydrofluoric acid before subsequent DLTS measurements. About 50–60 nm thickness of the epilayers was consumed by the oxidation process.

III. RESULTS AND DISCUSSION

A. Deep levels in n-type 4H-SiC/6H-SiC after low-energy electron irradiation

The Z_1/Z_2 and EH6/7 centers were predominantly observed in the as-grown 4H-SiC epilayers used in this study. The trap concentrations were typically $2.1 \times 10^{13} \text{ cm}^{-3}$ for the Z_1/Z_2 center and $1.3 \times 10^{13} \text{ cm}^{-3}$ for the EH6/7 center, respectively. Figure 1 shows the DLTS spectra of 4H-SiC after the e^- -irradiation with various electron fluences. Here, the signal b_1 is the coefficient of the first sine term in the Fourier series of deep level transient Fourier spectroscopy.²³

TABLE I. Electrical properties of the detected traps in electron-irradiated n-type 4H-SiC (σ : capture cross section, N_T : trap concentration after the e^- -irradiation with a fluence of $4 \times 10^{17} \text{ cm}^{-2}$).

Label	σ (cm^2)	$E_C - E_T$ (eV)	N_T (cm^{-3})
EH1	10^{-15}	0.36	8.5×10^{13}
Z_1/Z_2	10^{-14}	0.65	6.5×10^{14}
EH3	10^{-14}	0.79	1.9×10^{14}
EH5	10^{-16}	1.0	3.1×10^{13}
EH6/7	10^{-14}	1.48	4.1×10^{14}

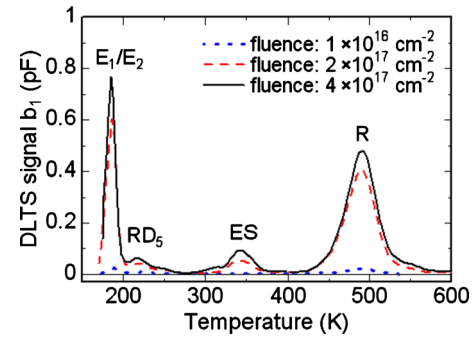


FIG. 2. (Color online) DLTS spectra of as-irradiated n-type 6H-SiC. Electron irradiation was performed at an energy of 150 keV with fluences of 1×10^{16} , 2×10^{17} , and $4 \times 10^{17} \text{ cm}^{-2}$.

The concentrations of the Z_1/Z_2 and EH6/7 centers were significantly increased by the e^- -irradiation. After the e^- -irradiation, three DLTS peaks, labeled EH1, EH3, and EH5,⁴ appeared in the measured temperature range. From the Arrhenius plots of the emission time constants, the energy levels and the capture cross-sections of the observed five traps were determined, which are summarized in Table I. The EH1, EH3, and EH5 centers are thermally unstable traps, while the Z_1/Z_2 and EH6/7 centers are thermally stable traps. Subsequent annealing at 950 °C completely removed the EH1, EH3, and EH5 peaks in DLTS spectra. On the other hand, the concentrations of the Z_1/Z_2 and EH6/7 centers were kept almost constant before and after annealing at 950 °C. These results are in accordance with the previous reports.^{9,10}

In the as-grown 6H-SiC epilayers used in this study, the E_1/E_2 center³ ($E_C - 0.45 \text{ eV}$) and the R center³ ($E_C - 1.25 \text{ eV}$) were observed. The typical trap concentrations were $2.3 \times 10^{12} \text{ cm}^{-3}$ for the E_1/E_2 center and $4.5 \times 10^{12} \text{ cm}^{-3}$ for the R center, respectively. The DLTS spectra of 6H-SiC after the e^- -irradiation are shown in Fig. 2. It was confirmed that the E_1/E_2 and R concentrations were significantly increased by low-energy electron irradiation. Two DLTS peaks, labeled RD_5 ³ and ES in the figure, were detected in the DLTS spectra of as-irradiated 6H-SiC. These two traps were not observed in the as-grown samples. The energy levels and the capture cross-sections of the detected four traps are summarized in Table II. Several groups observed a relatively broad peak, named Z_1/Z_2 (6H), at around 340 K in DLTS spectra of irradiated 6H-SiC.^{3,15–17,19–21} The Z_1/Z_2 center (6H) is not the same as the Z_1/Z_2 center in 4H-SiC, though the same label has been given. The Z_1/Z_2 center (6H) is located at about 0.6 eV below the conduction

TABLE II. Electrical properties of the detected traps in electron-irradiated n-type 6H-SiC (σ : capture cross section, N_T : trap concentration after the e^- -irradiation with a fluence of $4 \times 10^{17} \text{ cm}^{-2}$).

Label	σ (cm^2)	$E_C - E_T$ (eV)	N_T (cm^{-3})
E_1/E_2	10^{-12}	0.45	6.0×10^{14}
RD_5	10^{-13}	0.57	4.7×10^{13}
ES	10^{-14}	0.80	8.8×10^{13}
R	10^{-13}	1.25	5.1×10^{14}

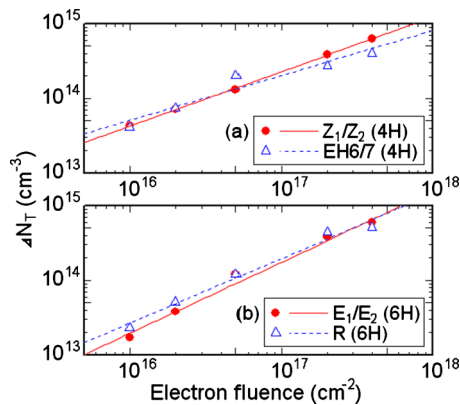


FIG. 3. (Color online) Dependence of increase in (a) Z_1/Z_2 and EH6/7 concentrations (ΔN_T) in n-type 4H-SiC and (b) E_1/E_2 and R concentrations (ΔN_T) in n-type 6H-SiC by the electron irradiation on the electron fluence (e^- -energy: 150 keV).

band edge in the band gap. The ES center observed in this study has a slightly larger activation energy than that of the Z_1/Z_2 center (6H), though both trap peaks were detected at similar temperature positions in the DLTS spectra. The previous annealing studies of the Z_1/Z_2 center (6H) have shown contradictory results: the defect center is persisting even after 1700 °C annealing,^{3,16} or annealed out below 1000 °C.^{17–19,21} In this study, the ES center were completely annealed out by annealing at 950 °C. At present, it is not clear whether the ES center is identical to the Z_1/Z_2 center (6H) or not. In any cases, the ES center may be related to carbon displacement. The RD_5 center is also thermally unstable as the ES center, while the E_1/E_2 and R centers remained stable after subsequent annealing at 950 °C. The RD_5 and ES centers in 6H-SiC have the similar features as the EH1, EH3, and EH5 centers in 4H-SiC: all these traps are not observed in as-grown epilayers, generated by the e^- -irradiation, and annealed out at relatively low temperature. Recent *ab initio* calculation has shown that migration barriers of a carbon vacancy (3.5–5.2 eV) are much higher than those of a carbon interstitial (0.5–1.4 eV) in SiC.²⁵ Zolnai *et al.* reported that the carbon vacancy in e^- -irradiated SiC becomes mobile at temperatures above 1100 °C as detected by electron spin resonance experiments.²⁶ Taking account of these theoretical and experimental results, the authors speculate that the EH1, EH3, and EH5 centers in 4H-SiC and the RD_5 and ES centers in 6H-SiC may be related to carbon interstitials.

Figures 3(a) and 3(b) show the increase in the concentrations of thermally stable traps, the Z_1/Z_2 , EH6/7 centers in 4H-SiC, and the E_1/E_2 , R centers in 6H-SiC, respectively. In these figures, the increases in trap concentrations are plotted versus the electron fluence. As can be seen, the Z_1/Z_2 , EH6/7, E_1/E_2 , and R concentrations were increased almost linearly by increasing the electron fluence. The generation rates of all these four traps by the e^- -irradiation are almost the same. This result suggest that the Z_1/Z_2 , EH6/7, E_1/E_2 and R centers originate from the same or a very similar point defect, which will be most likely a carbon vacancy.

In the same way, the authors compared the increase in the concentrations of thermally unstable traps, the EH1, EH3, EH5 centers in 4H-SiC, and the RD_5 , ES centers in

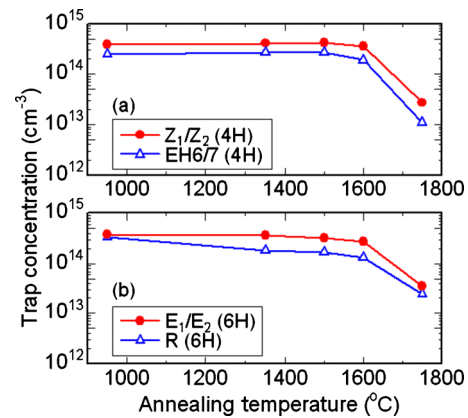


FIG. 4. (Color online) Annealing temperature dependence of trap concentrations for (a) the Z_1/Z_2 , EH6/7 centers in n-type 4H-SiC and (b) the E_1/E_2 , R centers in n-type 6H-SiC. Electron irradiation (energy: 150 keV, fluence: $2 \times 10^{17} \text{ cm}^{-2}$) was performed before each annealing.

6H-SiC. However, most of them did not show linear increase by increasing the electron fluence. Since these trap concentrations were changed even after the DLTS measurement up to 700 K, the annealing effect during the high-temperature measurements might affect their concentrations.

B. Further comparison of thermally stable traps observed in 4H-SiC/6H-SiC

As mentioned in the previous section, the Z_1/Z_2 , EH6/7 centers in 4H-SiC and the E_1/E_2 , R centers in 6H-SiC are dominant traps after the e^- -irradiation and subsequent annealing at 950 °C. In this section, the authors attempted further comparison of these thermally stable traps. As the first step, annealing at elevated temperatures up to 1750 °C were performed. As already mentioned, carbon caps were first deposited onto the sample surface before each annealing procedure. There was no sign of surface roughening in all the samples even after annealing at 1750 °C. Figure 4(a) shows the annealing behaviors of the Z_1/Z_2 and EH6/7 centers in 4H-SiC. The samples were irradiated with electrons (energy: 150 keV, fluence: $2 \times 10^{17} \text{ cm}^{-2}$) before annealing to introduce moderate amounts of the defect centers. The Z_1/Z_2 and EH6/7 concentrations were not changed by annealing at 1500 °C and decreased at higher temperature. The thermal stability of these defect centers are in good agreement with previous reports.^{9,11,27,28} Figure 4(b) shows the annealing behaviors of the E_1/E_2 and R centers in 6H-SiC. Before annealing, the samples were also irradiated with the same conditions as performed on the 4H-SiC samples used in this annealing experiment. The E_1/E_2 and R centers also remained stable up to 1500 °C and started to be annealed out at 1600–1750 °C. Comparing Figs. 4(a) and 4(b), it is obvious that the concentrations of the Z_1/Z_2 , EH6/7, E_1/E_2 , and R centers are changed in a very similar manner by high-temperature annealing. Such high thermal stabilities indicate that these defect centers are related to a carbon vacancy (or an antisite) rather than a carbon interstitial.

The authors also investigated effects of thermal oxidation on these four traps. It has been previously shown that the concentrations of the Z_1/Z_2 and EH6/7 centers can be

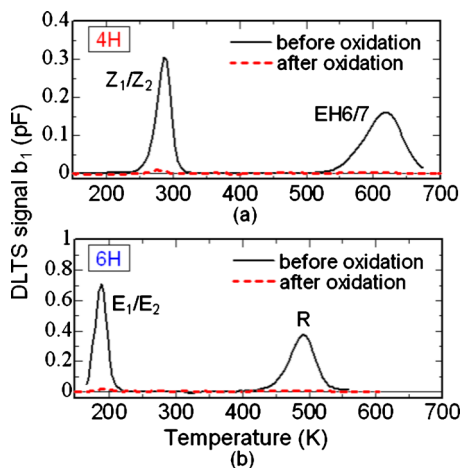


FIG. 5. (Color online) DLTS spectra of n-type (a) 4H-SiC and (b) 6H-SiC before and after thermal oxidation at 1150 °C for 6 h. Before oxidation, samples were irradiated with electrons (energy: 150 keV, fluence: $2 \times 10^{17} \text{ cm}^{-2}$) and annealed at 950 °C.

remarkably reduced by thermal oxidation.²⁹ The authors' group suggested a model for the mechanism of defect reduction: vacancy-related defects, likely the origins of the Z_1/Z_2 and EH6/7 centers, are occupied by diffused carbon or silicon interstitials emitted from the oxidation interface during thermal oxidation.³⁰ If the E_1/E_2 and R centers in 6H-SiC originate from the same microstructures as the Z_1/Z_2 and EH6/7 centers in 4H-SiC, their concentrations must be reduced by thermal oxidation in a same way. In this study, the authors conducted thermal oxidation in dry O_2 at 1150 °C for 6 h. The samples used in this experiment were irradiated with electrons (energy: 150 keV, fluence: $2 \times 10^{17} \text{ cm}^{-2}$) and annealed at 950 °C in Ar. Before oxidation, the samples contained only the Z_1/Z_2 center ($3.9 \times 10^{14} \text{ cm}^{-3}$) and the EH6/7 center ($2.5 \times 10^{14} \text{ cm}^{-3}$) in 4H-SiC, and the E_1/E_2 center ($3.8 \times 10^{14} \text{ cm}^{-3}$) and the R center ($3.3 \times 10^{14} \text{ cm}^{-3}$) in 6H-SiC. Figure 5(a) depicts the DLTS spectra of 4H-SiC before and after thermal oxidation. In accordance with the previous reports,^{29–31} the Z_1/Z_2 and EH6/7 centers were significantly reduced by thermal oxidation. Figure 5(b) depicts the DLTS spectra of 6H-SiC before and after thermal oxidation. As can be seen in the figure, the E_1/E_2 and R centers were also remarkably reduced by thermal oxidation. The changes in the trap concentrations are summarized in Table III. Under the present oxidation condition, the concentrations of the Z_1/Z_2 , EH6/7, E_1/E_2 , and R centers were reduced by more than one order of magnitude. Longer oxidation time or higher oxidation temperature would result in further elimination of these four traps. The

TABLE III. Trap concentrations of the Z_1/Z_2 , EH6/7 centers in n-type 4H-SiC, and the E_1/E_2 , R centers in n-type 6H-SiC before and after thermal oxidation at 1150 °C for 6 h.

	N_T (before oxidation)	N_T (after oxidation)
Z_1/Z_2 (4H)	$3.9 \times 10^{14} \text{ cm}^{-3}$	$1.2 \times 10^{13} \text{ cm}^{-3}$
EH6/7 (4H)	$2.5 \times 10^{14} \text{ cm}^{-3}$	$5.7 \times 10^{12} \text{ cm}^{-3}$
E_1/E_2 (6H)	$3.8 \times 10^{14} \text{ cm}^{-3}$	$1.7 \times 10^{13} \text{ cm}^{-3}$
R (6H)	$3.3 \times 10^{14} \text{ cm}^{-3}$	$4.3 \times 10^{12} \text{ cm}^{-3}$

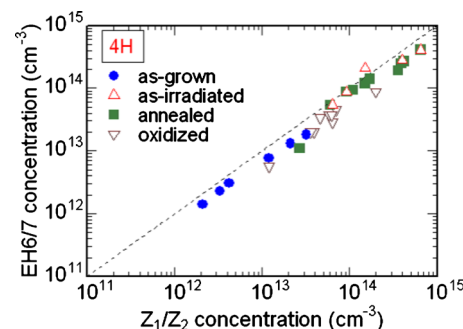


FIG. 6. (Color online) The relation between the Z_1/Z_2 and EH6/7 concentrations in n-type 4H-SiC obtained for as-grown samples, as-irradiated samples (e^- -energy: 150 keV), samples annealed at various temperatures (after e^- -irradiation at 150 keV), samples oxidized at 1150 °C (after e^- -irradiation at 150 keV with several fluences and annealing at 950 °C).

authors confirmed that the concentrations of the Z_1/Z_2 , EH6/7, E_1/E_2 , and R centers exhibit a very similar depth profile in the depth from 0.6 to 2.5 μm .

The observed results in this section support the hypothesis that the Z_1/Z_2 , EH6/7, E_1/E_2 , and R centers originate from the same microstructures, and they are probably related to a carbon vacancy. Figure 6 shows the relation between Z_1/Z_2 and EH6/7 concentrations in 4H-SiC epilayers after various processes obtained in this study. In accordance with the previous report,⁹ almost one-to-one correlation was observed for the Z_1/Z_2 and EH6/7 concentrations in 4H-SiC. One possible explanation is that these defect centers originate from the same microstructure with different charge states. In Fig. 7, the relation between E_1/E_2 and R concentrations in 6H-SiC epilayers is presented. The concentrations of the E_1/E_2 and R centers in 6H-SiC are almost the same for as-grown, electron-irradiated, annealed, and oxidized samples. From this result, the E_1/E_2 and R center may be also attributed to the same origin but different charge states, though further careful investigations are required.

C. Discussion

Figure 8 shows the relation between Z_1/Z_2 concentration in 4H-SiC epilayers and E_1/E_2 concentration in 6H-SiC epilayers obtained for as-grown, electron-irradiated, annealed, and oxidized samples. Here, each process was simulta-

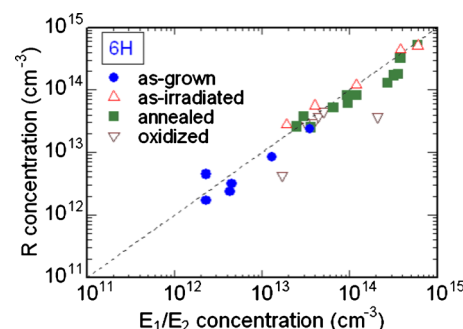


FIG. 7. (Color online) The relation between the E_1/E_2 and R concentrations in n-type 6H-SiC obtained for as-grown samples, as-irradiated samples (e^- -energy: 150 keV), samples annealed at various temperatures (after e^- -irradiation at 150 keV), samples oxidized at 1150 °C (after e^- -irradiation at 150 keV with several fluences and annealing at 950 °C).

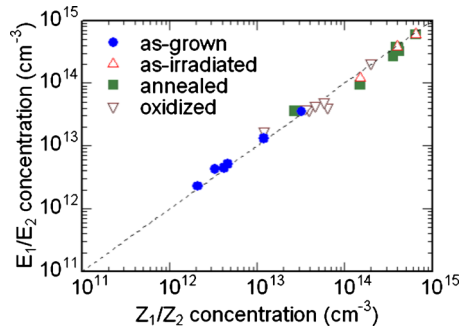


FIG. 8. (Color online) The relation between the concentrations of the Z_1/Z_2 center in n-type 4H-SiC and the E_1/E_2 center in n-type 6H-SiC obtained for as-grown samples, as-irradiated samples (e^- -energy: 150 keV), samples annealed at various temperatures (after e^- -irradiation at 150 keV), samples oxidized at 1150 °C (after e^- -irradiation at 150 keV with several fluences and annealing at 950 °C).

neously conducted for the 4H-SiC and 6H-SiC epilayers side by side. As can be seen in the figure, the concentrations of these defect centers are almost the same each other after the same processes. In the same way, EH6/7 concentration in 4H-SiC epilayers and R concentration in 6H-SiC epilayers are almost the same for as-grown, electron-irradiated, annealed, and oxidized samples, as shown in Fig. 9. Thus, generation and reduction processes are almost identical between the Z_1/Z_2 center in 4H-SiC and the E_1/E_2 center in 6H-SiC, and between the EH6/7 center in 4H-SiC and the R center in 6H-SiC. It should be noted that the generation of all these defects in as-grown epilayers is enhanced under Si-rich (low C/Si ratio) condition, and the defect concentrations decrease under C-rich (high C/Si ratio) condition. This result is consistent with a model that these defects originate from a carbon vacancy rather than a carbon interstitial.

The authors compared the energy positions of the defect centers observed in this study in the band gap. In Fig. 10, the energy positions of thermally stable traps investigated in this study are shown, considering the valence band alignment of different polytypes³² and a band gap offset between 4H-SiC (3.26 eV) and 6H-SiC (3.02 eV). As shown in Fig. 10, there are one-to-one correlations of deep levels in 4H-SiC and 6H-SiC. The Z_1/Z_2 center and the E_1/E_2 center are located at close energy positions from the valence band maxima. In

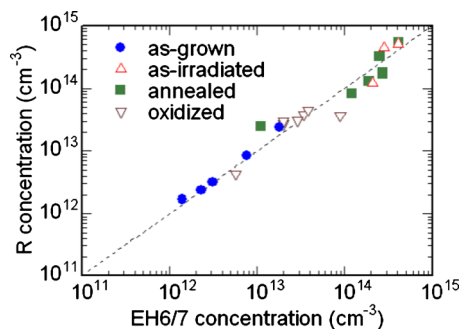


FIG. 9. (Color online) The relation between the concentrations of the EH6/7 center in n-type 4H-SiC and the R center in n-type 6H-SiC obtained for as-grown samples, as-irradiated samples (e^- -energy: 150 keV), samples annealed at various temperatures (after e^- -irradiation at 150 keV), samples oxidized at 1150 °C (after e^- -irradiation at 150 keV with several fluences and annealing at 950 °C).

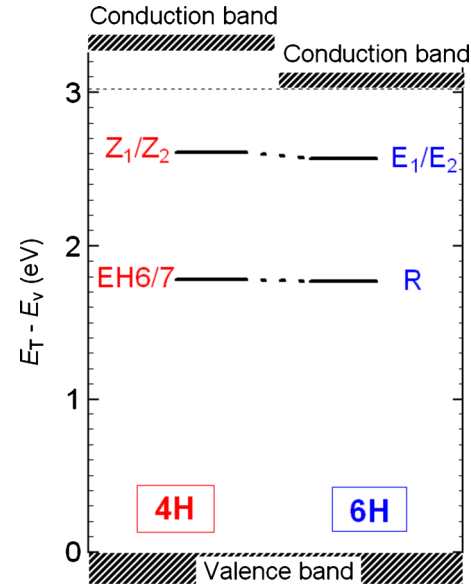


FIG. 10. (Color online) Energy positions in the band gap of thermally stable traps, the Z_1/Z_2 and EH6/7 centers in n-type 4H-SiC, and the E_1/E_2 and R centers in n-type 6H-SiC.

the same way, the EH6/7 centers are closely located as the R center. Taking account of the energy positions and features of the defect centers, the authors suggest that the Z_1/Z_2 center in 4H-SiC corresponds to the E_1/E_2 center in 6H-SiC, and the EH6/7 center in 4H-SiC to the R center in 6H-SiC, respectively. It was also suggested that the Z_1/Z_2 center in 4H-SiC corresponds to the E_1/E_2 center in 6H-SiC, judging from their similar annealing stages^{11,12} and negative-U properties.^{13,14} Langer and Heinrich showed that the energy levels related to transition metal impurities are aligned for the same group of isovalent semiconducting compounds (e.g., III-V and II-VI compounds).³³ Dalibor *et al.* suggested that the Langer-Heinrich rule is applicable to the Ti-related deep levels in SiC polytypes.³⁴ Grillenberger *et al.* reported the energy level alignment of the Ta-related deep levels in the band gap of the three polytypes 4H-SiC, 6H-SiC, and 15R-SiC.³⁵ The results observed in this work indicate that the Langer-Heinrich rule is also valid for the intrinsic defects in different SiC polytypes.

The authors observed similar correspondence for thermally unstable traps, the EH1, EH3, and EH5 centers in 4H-SiC and the RD₅ and ES centers in 6H-SiC. In Fig. 11, the energy positions of these thermally unstable traps are shown. Judging from the energy positions, the EH3 center in 4H-SiC may correspond to the RD₅ center in 6H-SiC, and the EH5 center in 4H-SiC to the ES center in 6H-SiC, respectively. In Fig. 11, the EH1 center in 4H-SiC seems to have no counterpart in 6H-SiC, but the authors speculate that another DLTS peak can be detected in a DLTS spectrum of irradiated 6H-SiC at lower temperature than 150 K. In the previous reports,^{3,18,20} one trap, named ED1, has been observed at around 120 K in DLTS spectra of irradiated 6H-SiC. The ED1 center is energetically located at about 0.2 eV below the conduction band edge. The ED1 center in 6H-SiC may correspond to the EH1 center in 4H-SiC. Further investigations, such as more detailed annealing study, are required before making conclusive remark.

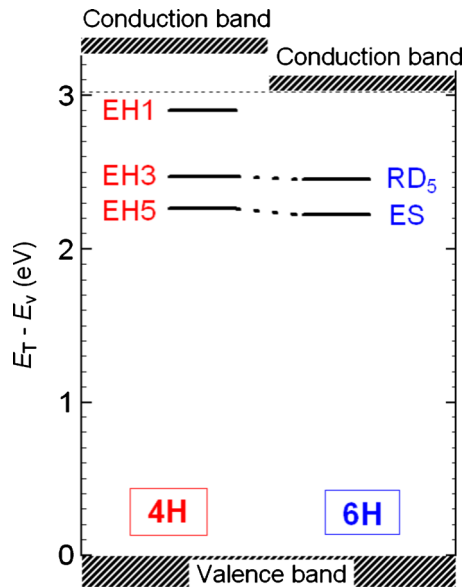


FIG. 11. (Color online) Energy positions in the band gap of thermally unstable traps, the EH1, EH3, and EH5 centers in n-type 4H-SiC and the RD₅ and ES centers in n-type 6H-SiC.

IV. SUMMARY

After low-energy electron irradiation, the authors detected five traps in 4H-SiC, and four traps in 6H-SiC. The Z₁/Z₂ and EH6/7 centers in 4H-SiC and the E₁/E₂ and R centers in 6H-SiC were dominant traps after the subsequent annealing. These four traps showed several similar features: their generation rates by the e⁻-irradiation were almost the same each other. The annealing behaviors of these traps are very similar, stable up to 1500 °C and being annealed above 1650 °C. In addition, thermal oxidation significantly reduced their concentrations. The generation of these defects during epitaxial growth is enhanced under Si-rich condition. These results may indicate that the Z₁/Z₂, EH6/7, E₁/E₂, and R centers originate from a microscopically same defect, most likely carbon vacancy. By considering the close energy positions in the band gap, the authors suggest that the Z₁/Z₂ center in 4H-SiC corresponds to the E₁/E₂ center in 6H-SiC, and the EH6/7 center in 4H-SiC to the R center in 6H-SiC, respectively. The authors also observed similar correspondence for thermally unstable traps in 4H-SiC and 6H-SiC. The EH3 center in 4H-SiC may correspond to the RD₅ center in 6H-SiC, and the EH5 center in 4H-SiC to the ES center in 6H-SiC, respectively. These results indicate that the Langer-Heinrich rule is also valid for the intrinsic defects in different SiC polytypes.

ACKNOWLEDGMENTS

This work was supported by a Grant-in-Aid for Scientific Research (Grant No. 21226008) from the Japan Society

for the Promotion of Science, and the Global COE Program (Grant No. C09) from the Ministry of Education, Culture, Sports and Technology, Japan.

- ¹R. F. Davis, G. Kelner, M. Shur, J. W. Palmour, and J. A. Edmond, *Proc. IEEE* **79**, 677 (1991).
- ²H. Matsunami and T. Kimoto, *Mater. Sci. Eng. R.* **20**, 125 (1997).
- ³T. Dalibor, G. Pensl, H. Matsunami, T. Kimoto, W. J. Choyke, A. Schöner, and N. Nordell, *Phys. Status Solidi A* **162**, 199 (1997).
- ⁴C. Hemmingsson, N. T. Son, O. Kordina, J. P. Bergman, E. Janzén, J. L. Lindström, S. Savage, and N. Nordell, *J. Appl. Phys.* **81**, 6155 (1997).
- ⁵K. Danno, D. Nakamura, and T. Kimoto, *Appl. Phys. Lett.* **90**, 202109 (2007).
- ⁶P. B. Klein, *J. Appl. Phys.* **103**, 033702 (2008).
- ⁷T. Tawara, H. Tsuchida, S. Izumi, I. Kamata, and K. Izumi, *Mater. Sci. Forum* **457–460**, 565 (2004).
- ⁸S. A. Reshanov, W. Bartsch, B. Zippelius, and G. Pensl, *Mater. Sci. Forum* **615–617**, 699 (2009).
- ⁹K. Danno and T. Kimoto, *J. Appl. Phys.* **100**, 113728 (2006).
- ¹⁰L. Storasta, J. P. Bergman, E. Janzén, A. Henry, and J. Lu, *J. Appl. Phys.* **96**, 4909 (2004).
- ¹¹M. Weidner, T. Frank, G. Pensl, A. Kawasuso, H. Itoh, and R. Krause-Rehberg, *Physica B* **308–310**, 633 (2001).
- ¹²G. Pensl, T. Frank, M. Krieger, M. Laube, S. Reshanov, F. Schmid, and M. Weidner, *Physica B* **340–342**, 121 (2003).
- ¹³C. G. Hemmingsson, N. T. Son, A. Ellison, J. Zhang, and E. Janzén, *Phys. Rev. B* **58**, R10119 (1998).
- ¹⁴C. G. Hemmingsson, N. T. Son, and E. Janzén, *Appl. Phys. Lett.* **74**, 839 (1999).
- ¹⁵C. Hemmingsson, N. T. Son, O. Kordina, E. Janzén, and J. L. Lindström, *J. Appl. Phys.* **84**, 704 (1998).
- ¹⁶G. Pensl and W. J. Choyke, *Physica B* **185**, 264 (1993).
- ¹⁷J. P. Doyle, M. O. Aboelfotoh, B. G. Svensson, A. Schöner, and N. Nordell, *Diamond Relat. Mater.* **6**, 1388 (1997).
- ¹⁸M. Gong, S. Fung, C. D. Beling, and Z. You, *J. Appl. Phys.* **85**, 7604 (1999).
- ¹⁹M. O. Aboelfotoh and J. P. Doyle, *Phys. Rev. B* **59**, 10823 (1999).
- ²⁰X. D. Chen, C. L. Yang, M. Gong, W. K. Ge, S. Fung, C. D. Beling, J. N. Wang, M. K. Lui, and C. C. Ling, *Phys. Rev. Lett.* **92**, 125504 (2004).
- ²¹C. C. Ling, X. D. Chen, G. Brauer, W. Anwand, W. Skorupa, H. Y. Wang, and H. M. Weng, *J. Appl. Phys.* **98**, 043508 (2005).
- ²²T. Kimoto, A. Itoh, and H. Matsunami, *Phys. Status Solidi B* **202**, 247 (1997).
- ²³S. Weiss and R. Kassing, *Solid-State Electron.* **31**, 1733 (1988).
- ²⁴Y. Negoro, K. Katsumoto, T. Kimoto, and H. Matsunami, *J. Appl. Phys.* **96**, 224 (2004).
- ²⁵M. Bockstedte, A. Mattausch, and O. Pankratov, *Phys. Rev.* **69**, 235202 (2004).
- ²⁶Z. Zolnai, N. T. Son, C. Hallin, and E. Janzén, *J. Appl. Phys.* **96**, 2406 (2004).
- ²⁷Y. Negoro, T. Kimoto, and H. Matsunami, *Appl. Phys. Lett.* **85**, 1716 (2004).
- ²⁸G. Alfieri, E. V. Monakhov, B. G. Svensson, and M. K. Linnarsson, *J. Appl. Phys.* **98**, 043518 (2005).
- ²⁹T. Hiyoshi and T. Kimoto, *Appl. Phys. Express* **2**, 041101 (2009).
- ³⁰T. Hiyoshi and T. Kimoto, *Appl. Phys. Express* **2**, 091101 (2009).
- ³¹K. Kawahara, J. Suda, G. Pensl, and T. Kimoto, *J. Appl. Phys.* **108**, 033706 (2010).
- ³²V. V. Afanas'ev, M. Bassler, G. Pensl, M. J. Schulz, and E. S. von Kaminski, *J. Appl. Phys.* **79**, 3108 (1996).
- ³³J. M. Langer and H. Heinrich, *Phys. Rev. Lett.* **55**, 1414 (1985).
- ³⁴T. Dalibor, G. Pensl, N. Nordell, and A. Schöner, *Phys. Rev. B* **55**, 13618 (1997).
- ³⁵J. Grillenberger, G. Pasold, W. Witthuhn, and N. Achtziger, *Appl. Phys. Lett.* **79**, 2405 (2001).